

Identity of long-range surface plasmons along asymmetric structures and their potential for refractometric sensors

F. Pigeon^{a)}

Laboratoire TSI, U.M.R. C.N.R.S. 5516, 42023 Saint-Etienne cedex, France

I. F. Salakhutdinov^{b)}

General Physics Institute of the Russian Academy of Sciences, 117942 Moscow, Russia

A. V. Tishchenko^{c)}

Laboratoire TSI, U.M.R. C.N.R.S. 5516, 42023 Saint-Etienne cedex, France

(Received 8 January 2001; accepted for publication 24 April 2001)

The field identity of the long-range surface plasmon (LRSP) mode in an asymmetric metal dielectric structure is elucidated and it is shown that it can be pictured as having a zero crossing of the longitudinal electric field at the middle of the metal film. A parametric dependence between the metal and the dielectric layer thicknesses leading to a LRSP mode in an asymmetric structure is given. The sensitivity of an asymmetric four layer structure supporting a grating excited LRSP mode regarding sensing objectives has been investigated. It is compared with the sensitivity of a usual plasmon mode propagating along a metal–dielectric interface. The existence of an anomalous increase of the reflection coefficient in the case of the LRSP is observed theoretically and experimentally. The comparative study is made on the basis of analytical expressions which reveal that the LRSP does not bring a decisive advantage over the standard plasmon for sensor application but its specific features can be advantageously used once well understood. © 2001 American Institute of Physics. [DOI: 10.1063/1.1380407]

I. INTRODUCTION

A long search for long-range surface plasmons (LRSPs) has been pursued since Sarid¹ showed the possibility of their existence along a thin metallic slab embedded in a dielectric medium. It was initially thought that LRSPs can exist only in a near to symmetric structure. However, it was shown by Glasberg *et al.*² that a LRSP also exists in nonsymmetric structures provided the modal electric field can be made weak enough in the metal film.

The experimental evidence of LRSPs in both symmetrical and nonsymmetrical structures was given by Salakhutdinov *et al.*³ and Liao *et al.*⁴ and it was demonstrated that a LRSP can be used as a sensor mode.⁵ We first report here on the field identity of the LRSP mode in an asymmetric structure and give a parametric dependence between the metal and the dielectric layer thicknesses leading to a LRSP in an asymmetric structure. Secondly we report on further theoretical and experimental work aimed at evaluating the expected sensitivity of the LRSP for an evanescent wave sensor of the refractometric type.

II. THE LRSP ALONG A SYMMETRICAL STRUCTURE

Surface plasmons are collective longitudinal oscillations of electrons propagating along a metal–dielectric interface at optical frequencies.^{6,7} As the considered structure is homogeneous in one direction (*y* direction in Fig. 1), the electric

and magnetic fields do not depend on the *y* coordinate if the plane of incidence is chosen perpendicular to the *y* direction. The electromagnetic problem is therefore limited to the *x*-*z* plane. In addition, it suffices to consider the TM polarization field because a surface plasmon is necessarily a TM polarized wave. Consequently, the only field components involved are E_x , E_z , and H_y . The propagation and loss features of a LRSP can be best understood by considering the longitudinal electric field (E_x) because this component of the field is closely associated with the collective longitudinal oscillations of electrons. The fields of a plasmon mode are the largest at the metal–dielectric interfaces and decay exponentially into both media. The properties of surface plasmon modes propagating along a metal film depend on the film thickness h_m and on the permittivity of the adjacent dielectric media. When the metal is in the form of a thin film, there is one plasmon at each interface. In case the metal film is embedded symmetrically in a single dielectric material, the propagation constant of the plasmon modes propagating at either side of the metal film are equal. Decreasing the metal–film thickness h_m down to the field penetration depth in the metal makes the electromagnetic modal fields of the two surface waves overlap and the propagation constant splits into a large modal propagation constant β^+ (the longitudinal electric field component is symmetric and the magnetic field is asymmetric) and a smaller propagation constant β^- of a second order mode (the longitudinal electric field component is asymmetric and the magnetic field is symmetric). The three field components are represented in Fig. 1. The modal field components in the substrate, the metal film, and the cover are obtained by solving the dispersion equation and normalizing them to unit propagated power. In Fig. 1 as well

^{a)}Electronic mail: fpigeon@univ-st-etienne.fr

^{b)}Electronic mail: grating@univ-st-etienne.fr

^{c)}Electronic mail: ildar@kapella.gpi.ru

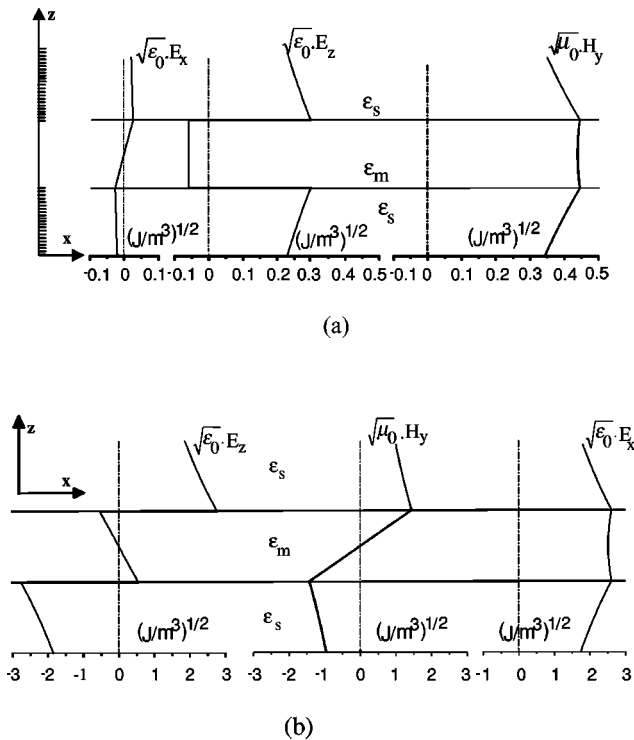


FIG. 1. Calculated and normalized surface plasmon field components along a symmetrical or quasi-symmetrical structure. (a) The LRSP (asymmetric longitudinal electric field of the plasmon mode of low propagation constant β^-) is presented. The scale on the z axis is decreased by a factor of 20 in the dielectric media. The metal is copper [the complex permittivity at 630 nm is taken from literature (see Ref. 14) and is equal to $(-11.33, 1.15)$], $h_m = 10$ nm and the cover and substrate is glass ($n=1.5$). (b) The short range surface plasmon (symmetric longitudinal electric field of the plasmon mode of large propagation constant β^+) is presented. The metal is copper $(-11.33, 1.15)$, $h_m = 10$ nm, and the cover and substrate is glass ($n=1.5$).

as in Fig. 2, all field components, which are normalized to unity propagated power, are expressed in the same mks units $(\text{Jm}^{-3})^{1/2}$ and are represented as $\sqrt{\epsilon_0}E$ and $\sqrt{\mu_0}H$. For a better graphic resolution in the metal layer, the scale was increased by 20 times on the z axis in the metal layer of Fig. 1(a).

It is worth noting that the dominant plasmon mode is the one exhibiting an antisymmetric dependence of its transverse field, unlike what prevails in dielectric waveguide modes. The complex propagation constants $\beta_x = \beta'_x + i\beta''_x$ of these two longitudinal electron oscillations are determined by the

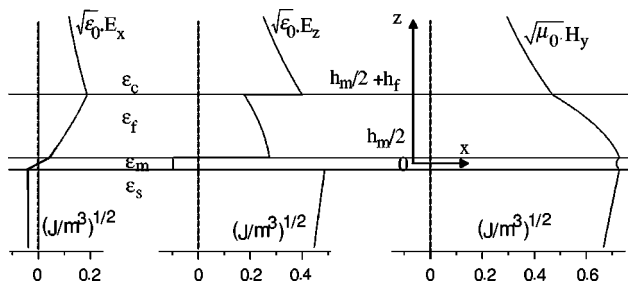


FIG. 2. Calculated and normalized long range surface plasmon field along a nonsymmetrical structure. The metal is copper $(-11.33, 1.15)$, $h_m = 10$ nm, the cover is water ($n=1.33$), the substrate is glass ($n=1.5$), the film is Si_3N_4 ($n=2$), and $h_f = 53.9$ nm.

dispersion relation resulting from the continuity condition on the tangential field components at both interfaces. The imaginary part β''_x is related with metal absorption. The power propagated by a surface plasmon along a smooth and flat surface decreases as $e^{-2\beta''_x}$. The values of β^+ and β^- depend on the complex permittivity of the metal film, of the surrounding medium, and especially on h_m . It was found in a study on the propagation constant in a symmetric device¹ that the damping of the low spatial frequency mode β^- (i.e., the mode with an asymmetric longitudinal electric field distribution) decreases with decreasing thickness h_m whereas the opposite occurs for the mode of propagation constant β^+ (i.e., the mode with a symmetric longitudinal electric field distribution). The physical reason is the decrease of the electric field in the metal film thus the decrease of dissipation by Joule losses. The amplitude of E_x in the metal decreases with the decrease of h_m since the E_x field extends further into the substrate as the mode gets closer to its cutoff ($h_m = 0$). The length L after which the intensity decreases to $1/e$ is proportional to $(2\beta'')^{-1}$, thus the propagation length of the second order mode increases with decreasing thickness h_m . A specific feature of the second order mode regarding propagation losses appears to be the zero crossing of the electron driving field at the middle of the metal film.

An analogic reasoning lets one anticipate that a long range character is expectable from a nonsymmetrical structure as well ($\epsilon_c \neq \epsilon_s$) (Fig. 2) provided the metal film is loaded by a dielectric layer of larger index at the cover side whose role is to shift the zero crossing of the longitudinal electric field towards the middle of the metal film.

III. THE LRSP ALONG A NONSYMMETRICAL STRUCTURE

In this section the parametric dependence between the metal thickness (h_m) and the dielectric layer thickness (h_f) (Fig. 2) leading to a LRSP in an asymmetric structure will be studied. There is no clear definition of what a long range plasmon mode should be. It is still the one of two modes whose electron driving field has a zero crossing within the metal film. The position of the zero of the E_x component on the z axis, and the resulting propagation loss, depend strongly on the dielectric load of the high index film. The dielectric thickness h_f and index n_f leading to the largest propagation length L can be determined by the four media dispersion equation (1) obtained by matching the tangent field components at the three boundaries of the structure. In analogy with the symmetric case, and with the concern of obtaining closed form analytical expressions for the sensing characteristics, we are defining here the LRSP structure as the one ensuring the zero crossing of the longitudinal electric field at the middle of the metal film. As will be shown later, this choice is physically plausible, and systematic numerical modeling shows that the actual field profile leading to the least propagation loss is very close to this condition.

Let us therefore assume that the minimum losses are obtained when the electric field component E_x has an antisymmetric distribution in the metal layer (Fig. 1). We will derive hereafter the condition which the structure parameters

must satisfy for this to happen. In this case, the tangent magnetic field component H_y has a symmetric distribution as illustrated in Figs. 1 and 2: $H_y|_{z=h_m/2} = H_y|_{z=-h_m/2}$ and its normal derivative is antisymmetric

$$\left. \frac{\partial H_y}{\partial z} \right|_{z=h_m/2} = - \left. \frac{\partial H_y}{\partial z} \right|_{z=-h_m/2}.$$

Dividing the second expression by the first one and by the metal permittivity ε_m yields the following expression:

$$\frac{1}{\varepsilon_m H_y} \left. \frac{\partial H_y}{\partial z} \right|_{z=h_m/2} = \frac{1}{\varepsilon_m H_y} \left. \frac{\partial H_y}{\partial z} \right|_{z=-h_m/2}. \quad (1)$$

The symmetric solution of the Maxwell equations is a hyperbolic cosine function in the metal film [see the Appendix, Eq. (A11)] if $|z| \leq h_m/2$. Therefore by substituting the expression of H_y , we can express a condition which has to be satisfied at the lower metal surface ($z = -h_m/2$) of the metal film

$$\frac{1}{\varepsilon_m H_y} \left. \frac{\partial H_y}{\partial z} \right|_{z=-h_m/2} = \frac{k \sqrt{n_e^2 - \varepsilon_m}}{\varepsilon_m} \tanh(k h_m \sqrt{n_e^2 - \varepsilon_m}), \quad (2)$$

where ε_s is the substrate permittivity and n_e is the effective index of the LRSPs.

The solution of Maxwell's equations is an exponential function in the substrate [see the Appendix Eq. (A11)] if $|z| \geq h_m/2$, so by substituting the expression of H_y in the continuity relation of the tangent component of the magnetic field at the lower metal interface ($z = -h_m/2$) we obtain

$$-\tanh\left(\frac{k h_m}{2} \sqrt{n_e^2 - \varepsilon_m}\right) = \frac{\varepsilon_m \sqrt{n_e^2 - \varepsilon_x}}{\varepsilon_s \sqrt{n_e^2 - \varepsilon_m}}. \quad (3)$$

A similar equation can be obtained at the upper metal surface ($z = h_m/2$), and since the product $1/\varepsilon H_y / \partial H_y / \partial z$ is continuous at both sides of an interface (because $1/\varepsilon \partial H_y / \partial z = j \omega E_x$), we obtain the needed thickness of the high refractive index layer h_f for the zero crossing of E_x at the middle of the metal film, i.e., under the above hypothesis for giving rise to LRSP in an asymmetric structure

$$k h_f \sqrt{\varepsilon_f - n_e^2} = M \pi + \arctan \frac{\varepsilon_f \sqrt{n_e^2 - \varepsilon_c}}{\varepsilon_c \sqrt{\varepsilon_f - n_e^2}} - \arctan \frac{\varepsilon_f \sqrt{n_e^2 - \varepsilon_s}}{\varepsilon_s \sqrt{\varepsilon_f - n_e^2}}, \quad (4)$$

where ε_f and ε_c are the permittivities of the dielectric layer and cover media, respectively, and h_f is the thickness of the dielectric layer. Equations (3) and (4) give the parametric dependence $h_f(h_m)$ of the LRSP in the asymmetric structure, that is, the thickness h_f which the dielectric must have to fulfill the condition of minimum propagation loss of the plasmon mode for a given metal thickness h_m .

This parametric dependence $h_f(h_m)$ of the dielectric film thickness was obtained under the hypothesis that the plasmon loss (i.e., the imaginary part of its effective index) is minimum when the E_x field component is zero at the middle of the metal film. The plausibility of this hypothesis will now

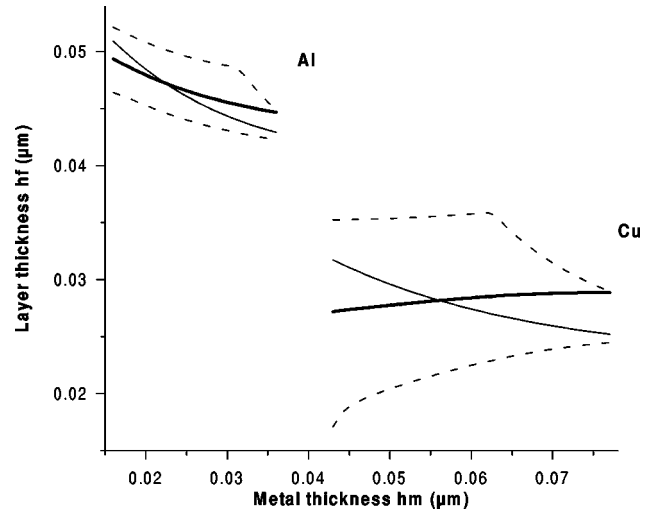


FIG. 3. The (h_m, h_f) pairs corresponding to a minimum absorption loss defined for a given metal (aluminum and copper were considered) curve in the (h_m, h_f) plane. These curves are given from the mode cutoff, i.e., h_m from 20 and 35 nm depending on the metal to about 100 nm. Exact thickness values (solid line) are accompanied with those given by the approximate expressions (3) and (4) (thinner line). The dashed lines correspond to (h_m, h_f) pairs leading to an imaginary part of the effective index which is 5% larger than the absolute minimum value.

be confirmed. The exact dispersion equation of the four-medium structure was first derived analytically. It was then solved numerically in the complex plane for a fixed metal thickness h_m with the objective of finding out the dielectric film thickness h_f leading to the least imaginary part of the effective index of the plasmon mode exhibiting a zero crossing of E_x . The (h_m, h_f) pairs leading to a minimum absorption loss define for a given metal (aluminum and copper were considered) a curve in the (h_m, h_f) plane extending from the mode cutoff, i.e., h_m from 20 and 35 nm depending on the metal to about 100 nm. These exact thickness values have been compared with those given by the approximate expressions (3) and (4) (see Fig. 3). A very good agreement can be found in all considered cases. This can be appreciated by realizing that the approximate h_f value given by Eq. (4) once substituted into the exact dispersion equation results in an imaginary part of the effective index which is hardly 5% larger than the absolute minimum value (Fig. 3). This teaches that first the field identity of the LRSP mode in an asymmetric structure involving a low loss metal film may be vividly pictured as having a zero crossing of E_x at the middle of the metal film and, secondly, that there is no strict existence condition for a LRSP: there is for each h_m a relative wide range of h_f values corresponding to bottom line losses. The calculated and normalized long range surface plasmon field components along the nonsymmetrical structure are presented in Fig. 2.

IV. GRATING EXCITATION OF A LRSP

The excitation of a surface plasmon requires a coupler (a grating coupler or a prism coupler), since the propagation constant lies above of the light line in the $\beta(\omega)$ dispersion diagram. We are concentrating here on the excitation of a long range surface plasmon by means of a grating. Unlike in

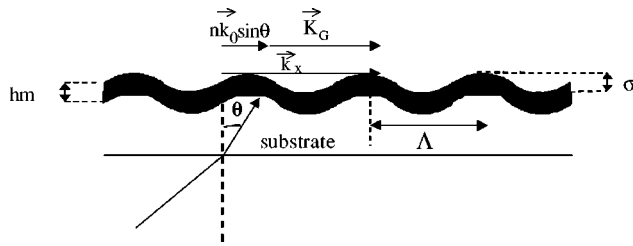


FIG. 4. Backside excitation of surface plasmons propagating along an ultrathin metal film deposited on a undulated substrate. Λ is the grating period and σ is the peak to valley amplitude.

the case of a grating coupled dielectric waveguide, the presence of the surface undulation represents a strong perturbation of the modal field and of the light guidance properties.

The grating acts as a coupler between an incident plane wave and the surface plasmon field. It diffracts light in different orders, one of which is used to couple the free-space wave to the plasmon. The spatial harmonics k_x along x of an incident beam impinging on a grating of period Λ at a resonant angle θ are given by the wave vectors: $k_x = \pm NK_G + k_{x0}$, where $k_{x0} = n_s \omega/c \sin \theta$ (c is the speed of electromagnetic waves in free space and ω is the optical frequency), $K_G = 2\pi/\Lambda$ and N is an integer which represents the diffraction order of the grating. Usually, a larger coupling efficiency is obtained by using the first diffraction order ($N=1$).

A plasmon propagating along an undulated metal slab exhibits losses due to the propagation along an absorptive medium, and experiences additional losses due to the field redistribution in the grating region. The plasmon mode also diffracts into plane waves in all possible diffraction orders at a rate which is described by the radiation coefficient α . If σ represents the groove depth (see Fig. 4), these losses (α) are proportional to σ^2 .³

The plasmon can be considered as a resonant mode with losses due to dissipation. The dissipation losses are described by α_{dis} which is the field decay rate along x . This resonator is open to the outside by the coupling grating. The efficiency of this coupler is proportional to α_{rad} . It is well known from the physics of open resonators⁸ that the optimum coupling is achieved when $\alpha_{\text{dis}} = \alpha_{\text{rad}}$. Therefore in order to have the maximum coupling of the incident wave energy into a plasmon mode, one has to find a balance between the radiation losses and the dissipative losses in the thin metal film. This condition can be satisfied by the appropriate choice of the grating amplitude σ .

V. ABNORMAL REFLECTION DUE TO THE EXISTENCE OF A LRSP

The excitation process of surface electromagnetic waves in a corrugated thin dielectric film was investigated theoretically and experimentally^{9,10} and led to the identification and observation of an anomalous increase of the reflection coefficient close to the excitation resonance.

If a light beam impinging onto the surface of a corrugated waveguide excites a waveguide mode, the modulus of the reflected beam can be much larger than the Fresnel reflection. The origin of this anomalously large reflection is the

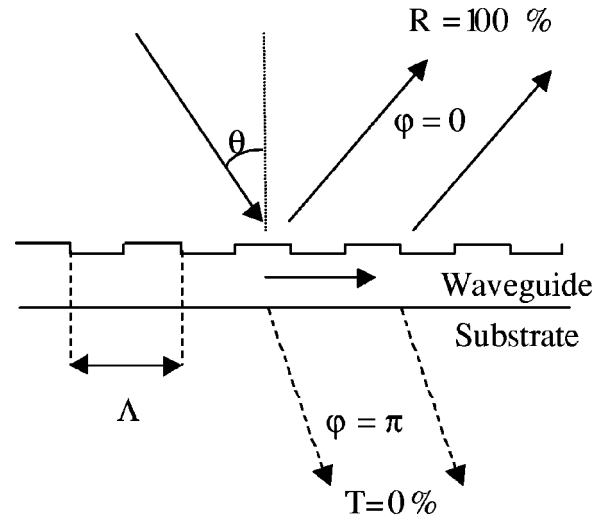


FIG. 5. Schematic representation of the effect of abnormal reflection on the corrugated surface of an optical dielectric waveguide.

interference between the light reflected from (or transmitted through) the surface of the waveguide and reradiated from the excited waveguide mode. Thus the necessary condition for obtaining a large effect is the excitation of a guided wave and the occurrence of light radiation into both media adjacent to the guiding layer.

Figure 5 is the symbolic representation of the conditions where the reflection coefficient (R) is equal to 100% (the reflected beam and the reradiated beam interfere constructively) and the transmission coefficient (T) is 0% (the transmitted beam and the reradiated beam interfere destructively).

The necessary conditions for the existence of abnormal light reflexion are⁹

$$\sin \theta \approx n_{\text{eff}} - \lambda/\Lambda,$$

$$D\alpha \gg 1, \quad (5)$$

$$\alpha_{\text{rad}} \gg \alpha_{\text{dis}},$$

where n_{eff} is the mode effective index, D is the incident beam diameter, and α is the total waveguide loss coefficient ($\alpha = \alpha_{\text{rad}} + \alpha_{\text{dis}}$).

For a plane incident wave and an infinite grating, the maximum achievable reflection coefficient (R_{inf}) is

$$R_{\text{inf}} = \frac{(\alpha_{\text{rad}} - R_F \alpha_{\text{dis}})^2}{(\alpha_{\text{rad}} + \alpha_{\text{dis}})^2}, \quad (6)$$

where R_F is the Fresnel reflection coefficient.

For a finite beam diameter D and a finite size grating of length L , the actual reflection coefficient (R_{fin}) is a function F :⁹ $R_{\text{fin}} = R_{\text{inf}} F(\alpha, \alpha_{\text{rad}}, D, L)$ where $F < 1$. In our case, we have found $R_{\text{fin}} \approx 50\%$ (α_{dis} cannot be completely compensated by α_{rad}).³

The necessary condition for obtaining this high reflection effect is the excitation of a guided wave and the occur-

rence of light radiation into both media adjacent to the guiding layer. A plasmon wave can also be considered as an analog of a guided wave in a dielectric film and we can expect the existence of an analogous effect for surface plasmons. If the corrugated metal film (Fig. 4) is thin enough, the incident light beam does not only reflect but is also partially transmitted through the metal film. An abnormal reflection effect is surely impossible to observe in structures which support the standard plasmon mode because of the high reflection coefficient from the metal film and its opacity. Another condition for abnormal reflection to take place is on the loss of the plasmon wave which should be smaller than its radiation rate along the corrugated interface. Long range plasmons can propagate with low dissipative losses. They are therefore good candidates for satisfying all the above conditions, therefore for exhibiting a large and sharp reflection peak.

VI. ABNORMAL REFLECTION FOR SENSOR OBJECTIVES

The asymmetric four layer structure is particularly interesting for evanescent wave refractometric or absorption sensors because, thanks to the additional dielectric layer, a long range plasmon can be made to propagate with an effective index close to and above the substrate index (usually glass or quartz) although the index of the cover (usually water or a solvent) is significantly lower. The penalty for this usability broadening is that the field at the interface with the measurand is less intense in the asymmetric four layer structure (Fig. 2) than in the standard plasmon case. This is, however, a necessary trade-off because the use of a symmetrical structure would considerably limit the range of possible cover materials and measurands. A comparative study is made here between three plasmon sensor schemes on the basis of analytical expressions. The comparison criteria will essentially be the sensitivity and the resolution. The three sensor schemes are a standard plasmon at a single metal–dielectric interface, a LRSP along a symmetrical structure and a LRSP in a nonsymmetrical structure. The sensitivity is the variation of the measurable variable angle of incidence θ upon the variation of the index of the cover. The resolution gives the smallest cover index increase leading to a measurable variation of θ . For sensing applications, these two characteristics are essential and different. For a specific application, one of them can be more important than the other.

The sensitivity S_{ne} of an evanescent sensor is defined as the variation of effective index n_e upon the variation of permittivity of the cover: $S_{ne} = \partial n_e / \partial(\Delta \epsilon \Delta h)$, where Δh is the thickness of the layer where the cover permittivity changes by $\Delta \epsilon$. An angular sensitivity S_θ can also be defined:

$$S_\theta = \frac{\partial \theta}{\partial(\Delta \epsilon \Delta h)} = \frac{1}{\cos \theta} \frac{\partial n_e}{\partial(\Delta \epsilon \Delta h)},$$

where θ is the angular position of the resonance ($\delta n_e = \cos \theta \delta \theta$).

The perturbation theory¹¹ gives a general expression for δn_e :

$$\delta n_e = \frac{1}{2n_e} \frac{\int_{-\infty}^{\infty} \frac{|H_y(z)|^2}{\epsilon(z)} \delta \epsilon(z) dz}{\int_{-\infty}^{\infty} \frac{|H_y(z)|^2}{\epsilon(z)} dz} \approx \frac{1}{2n_e} \frac{|H_y(z_0)|^2 \frac{\Delta \epsilon \Delta h}{\epsilon_c}}{\int_{-\infty}^{\infty} \frac{|H_y(z)|^2}{\epsilon(z)} dz}, \quad (7)$$

where H_y is the tangent magnetic field component. Equation (7) can be used to obtain a general expression for the angular sensitivity

$$S_\theta = \frac{1}{2n_e \cos \theta} \frac{\frac{|H_y(z_0)|^2}{\epsilon_c}}{\int_{-\infty}^{\infty} \frac{|H_y(z)|^2}{\epsilon(z)} dz}. \quad (8)$$

The waveguide power loss coefficient α_{dis} is proportional to the imaginary part of the effective index:

$$\alpha_{dis} = 2k_0 \text{Im}(n_e) \quad (9)$$

and the relative spectral width $\Delta \lambda / \lambda$ of the plasmon resonance is inversely proportional to the number N of grooves “seen” by the propagating longitudinal electric field E_x

$$N = \alpha_{dis} \Lambda. \quad (10)$$

Therefore

$$\frac{\Delta \lambda}{\lambda} = \frac{1}{2\pi N} = \frac{\alpha_{dis} \Lambda}{2\pi}. \quad (11)$$

The angular width $\Delta \theta$ of the plasmon resonance is determined by the plasmon mode losses

$$\Delta \theta = \frac{\alpha_{dis} \lambda}{2\pi \cos \theta} = \frac{2 \text{Im}(n_e)}{\cos \theta}. \quad (12)$$

The angular resolution R is the ratio between the angular sensitivity and the plasmon angular width

$$R \sim \frac{S_\theta}{\Delta \theta} = \frac{\text{Im}(n_e)}{2n_e \epsilon_c} \frac{|H_y(z_0)|^2}{\int_{-\infty}^{\infty} \frac{|H_y(z)|^2}{\epsilon(z)} dz}. \quad (13)$$

Analytical expressions (see the Appendix) have been obtained from the general expressions above for the sensitivity S_θ and for the resolution R in the case of a refractometric type sensor according to the three considered embodiments. The comparison between a sensor using a standard plasmon, a long range plasmon in a symmetrical structure, and a long range plasmon in a nonsymmetrical structure is presented in Table I.

Referring to Table I the parameter h_m (thickness of metal) is smaller than in the case of a standard plasmon in the case of a long range plasmon (in an asymmetric or symmetric structure). Therefore the sensitivity is larger for a standard plasmon setup. It can be noticed that the coefficient $[2\epsilon_c^2(\epsilon_f - \epsilon_s)] / [\epsilon_c^2(\epsilon_f - \epsilon_s) + \epsilon_f^2(\epsilon_s - \epsilon_c)]$ leads to a decrease of the sensitivity of a sensor based on a LRSP in an

TABLE I. Analytical expressions of the sensitivity S_θ and of the resolution R for a refractometric type sensor.

	Sensitivity	Resolution
Standard plasmon	$S_\theta \approx \frac{k_0}{\varepsilon_c^{1/2} \cos \theta} \frac{\text{Im} \sqrt{\varepsilon_m}}{ \varepsilon_m }$	$R \sim \frac{k_0}{\varepsilon_c^2} \frac{ \varepsilon_m }{2 \text{Re} \sqrt{\varepsilon_m}}$
LRSP in symmetrical structure	$S_\theta \approx \frac{k_0^2 h_m}{4 \cos \theta}$	$R \sim \frac{1}{2 \varepsilon_c^{5/2} h_m} \frac{ \varepsilon_m ^2}{\text{Im}(\varepsilon_m)}$
LRSP in nonsymmetrical structure	$S_\theta \approx \frac{k_0^2 h_m}{2 \cos \theta} \frac{\varepsilon_c^2 (\varepsilon_f - \varepsilon_s)}{\varepsilon_c^2 (\varepsilon_f - \varepsilon_s) + \varepsilon_f^2 (\varepsilon_s - \varepsilon_c)}$	$R \sim \frac{1}{\varepsilon_c^{5/2} h_m} \frac{ \varepsilon_m ^2}{\text{Im}(\varepsilon_m)} \frac{\varepsilon_c^2 (\varepsilon_f - \varepsilon_s)}{\varepsilon_c^2 (\varepsilon_f - \varepsilon_s) + \varepsilon_f^2 (\varepsilon_s - \varepsilon_c)}$

asymmetric structure in comparison with that of a symmetric structure. In the case of the experimental setup described in the next section ($n_s = 1.512$, $n_f = 1.81$, $\varepsilon_c = -8.24 + 2.2i$), this decrease coefficient is equal to 0.45. The decrease of the parameter h_m leads to an increase of the resolution of a long range plasmon sensing platform. The same coefficient $[2\varepsilon_c^2(\varepsilon_f - \varepsilon_s)]/[\varepsilon_c^2(\varepsilon_f - \varepsilon_s) + \varepsilon_f^2(\varepsilon_s - \varepsilon_c)]$ leads to a decrease of the resolution of a sensor based on a long range plasmon in an asymmetric structure in comparison with a sensor based on a long range plasmon in a symmetric structure.

Table II gives the relative merits of three sensor schemes on the basis of the sensitivity and the resolution and in the perspective of an abnormal reflection readout sensor scheme.

In conclusion, it can be said that the LRSP in a nonsymmetrical structure opens new possibilities for sensor applications. It was shown that LRSPs give rise to the possible new interrogation scheme using abnormal reflection which is a novel feature. This effect is very interesting for sensor applications because it makes it possible to monitor a maximum of optical power with high angular resolution instead of a broad dip. In standard plasmons the sensitivity is larger but it is spoiled by a lower angular resolution due to a larger resonance width; furthermore, the abnormal reflection effect is absent. Monitoring a resonance peak instead of a dip also implies a larger signal-to-noise ratio. The standard plasmon should, however, not be ruled out at all. Its practicality and its spatial multiplexing possibilities are very attractive and it has been demonstrated¹² that it can lead to high sensitive setup.

VII. EXPERIMENTAL RESULTS: LRSP IN A NONSYMMETRICAL STRUCTURE CAN BE USED AS A SENSOR PLATFORM

Long range plasmon excitation was performed on ultra-thin copper films deposited on corrugated glass substrates ($n_s = 1.512$). The gratings were first made on a glass substrate by standard holographic exposure with a He–Cd laser, followed by ion beam etching for the transfer of the grating from the resist film into the glass substrate (the grating period is $\Lambda = 0.37 \mu\text{m}$ and the groove depth is 56 nm). The resulting groove profile does not allow for the deposition of continuous thin metal films. Therefore the glass samples were annealed in a furnace at a temperature close to the glass softening temperature. The resulting profile is close to sinusoidal and allows for the deposition of continuous undulated metal films. Copper films [the complex permittivity at 630 nm was measured to be equal to $(-8.24, 2.2)$] were deposited by rf sputtering in a “Sputron-II” installation in an oil-less vacuum. The thickness was 10 nm. It was covered by a 116 nm thick Si_3N_4 film ($n_f = 1.81$).³ The characterization of such a structure was made at 630 nm wavelength with an air cover.

Figure 6 brings the experimental evidence of abnormal LRSP reflection. Two reflection peaks are observed which are caused by the LRSP excitation in two opposite directions. In spite of its relatively low anomalous reflection maximum, the long range plasmon exhibits its characteristic narrow angular width of reflection resonance. The result of a numerical modeling obtained by the rigorous method¹³ of the four layer

TABLE II. Characteristics comparison between Standard plasmon, LRSP in a symmetrical structure, and LRSP in a nonsymmetrical structure.

	Realizability of sensor setup	Sensitivity	Resolution	Abnormal reflection
Standard plasmon	possible	high	low	impossible
LRSP in symmetrical structure	impossible	average	high	possible
LRSP in nonsymmetrical structure	possible	low	high	possible

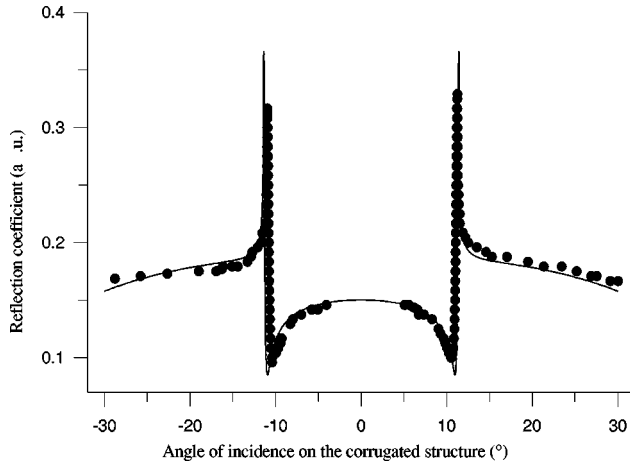


FIG. 6. Dependence of the reflection on the angle of incidence on the corrugated structure. The result of a numerical modeling obtained by the rigorous method (see Ref. 13) (solid line) of the four layer structure is compared with experimental results (circles). 10 nm of copper films [the complex permittivity at 630 nm was measured to be equal to $(-8.24, 2.2)$] was deposited. It was covered by a 116 nm thick Si_3N_4 film ($n_f=1.81$). The characterization was made at 630 nm wavelength with an air cover.

structure is compared with experimental results. It was shown by Liao *et al.*⁴ that a four-layer structure which supports LRSP modes can serve as a sensing platform. This structure is not very sensitive to the change of the cover's refractive index but has a good resolution (Table II and Fig. 6). It was experimentally demonstrated by Lyndin *et al.*⁵ that the LRSP can also allow the measurement of the properties of an ultrathin metal film.

VIII. CONCLUSION

The field identity of the LRSP mode in an asymmetric structure has been fully described. It is shown that it can be pictured as being characterized by a zero crossing of the longitudinal field at the middle of the metal film. The parametric dependence between the metal thickness (h_m) and the dielectric layer thickness (h_f) leading to a LRSP in an asymmetric structure is provided.

A theoretical comparison between a standard plasmon, a LRSP in a symmetrical structure, and a LRSP in a nonsymmetrical structure regarding evanescent wave sensing is presented. It is shown both theoretically and experimentally that a LRSP exhibits a definite abnormal reflection effect. This effect is practically interesting for sensor applications since it delivers a reflection maximum at synchronism with high angular resolution instead of the typical reflection dip of a standard plasmon. In a standard plasmon sensor the sensitivity is larger but it is spoiled by a lower angular resolution due to the larger resonance width.

A long range surface plasmon sensor is somewhere between a plasmon sensor and a dielectric waveguide sensor. Its propagation length and resonance width make it similar to the latter whereas its guidance and polarization pertain to the former. It is not clear whether this can be an advantage for practical applications. Its sensing sensitivity is lower than that of a plasmon sensor and its longer propagation length is not an advantage for high density spatial multiplexing of

sensor arrays. Concerning manufacturing technologies, the fabrication techniques of ultrathin metal films are not widely available and the need for the deposition of an additional dielectric film on the metal film is not favorable because one faces the same difficulty which the dielectric waveguide sensors meet, which is the chemical stability of dielectric film. The short-term prospects of LRSPs seem therefore mitigated although their existence in nonsymmetrical structures widely broadens their scope.

APPENDIX: DERIVATION OF ANALYTICAL EXPRESSIONS FOR THE SENSITIVITY AND RESOLUTION

1. Plasmon at a single interface

The transverse magnetic field component H_y of a plasmon propagating along a single metal–dielectric interface $z = z_0$ has the following transverse distribution:

$$H_y(x, z) = \begin{cases} H_0 \exp[ik_0 n_e x - k_0 \sqrt{n_e^2 - \epsilon_c}(z - z_0)], & z \geq z_0 \\ H_0 \exp[ik_0 n_e x + k_0 \sqrt{n_e^2 - \epsilon_m}(z - z_u)], & z \leq z_0 \end{cases} \quad (\text{A1})$$

where n_e is the plasmon effective index given by the explicit dispersion equation

$$n_e = \sqrt{\frac{\epsilon_c \epsilon_m}{\epsilon_c + \epsilon_m}}. \quad (\text{A2})$$

In the limit of large $|\epsilon_m|$ we can find from Eq. (13) and (14):

$$S_\theta \approx \frac{k_0}{\epsilon_c^{1/2} \cos \theta} \frac{\text{Im} \sqrt{\epsilon_m}}{|\epsilon_m|}, \quad (\text{A3})$$

$$\Delta \theta \approx \frac{\epsilon_c^{3/2}}{\cos \theta} \frac{\text{Im}(\epsilon_m)}{|\epsilon_m|^2}, \quad (\text{A4})$$

$$R \sim \frac{k_0}{\epsilon_c^2} \frac{|\epsilon_m|}{2 \text{Re} \sqrt{\epsilon_m}}. \quad (\text{A5})$$

2. Symmetrical long-range plasmon

The transverse magnetic field component H_y of a symmetrical long-range plasmon propagating along a thin metal film of thickness h_m has the following transverse distribution

$$H_y(x, z) = \begin{cases} H_0 \exp[ik_0 n_e x - k_0 \sqrt{n_e^2 - \epsilon_c}(|z| - h_m/2)], & |z| \geq h_m/2 \\ H_0 \exp(ik_0 n_e x) \frac{\cosh[k_0 \sqrt{n_e^2 - \epsilon_m} z]}{\cosh[k_0 \sqrt{n_e^2 - \epsilon_m} h_m/2]}, & |z| \leq h_m/2 \end{cases} \quad (\text{A6})$$

where n_e satisfies the dispersion equation

$$\epsilon_m \sqrt{n_e^2 - \epsilon_s} + \epsilon_s \sqrt{n_e^2 - \epsilon_m} \tanh \left[\frac{kh_m}{2} \sqrt{n_e^2 - \epsilon_m} \right] = 0. \quad (\text{A7})$$

In the limit of large $|\varepsilon_m|$ we can find from expressions (13) and (14)

$$S_0 \approx \frac{k_0^2 h_m}{4 \cos \theta}, \quad (\text{A8})$$

$$\Delta \theta \approx \frac{2\varepsilon_c^{5/2}}{\cos \theta} \left(\frac{k_0 h_m}{2} \right)^2 \frac{\text{Im}(\varepsilon_m)}{|\varepsilon_m|^2}, \quad (\text{A9})$$

$$R \sim \frac{1}{2\varepsilon_e^{5/2} h_m} \frac{|\varepsilon_m|^2}{\text{Im}(\varepsilon_m)}. \quad (\text{A10})$$

3. Long-range plasmon in a nonsymmetrical structure

Consider a plasmon propagating along a thin metal film of thickness h_m loaded by a dielectric film of high permittivity ε_f and thickness h_f placed between the metal film and the superstrate as illustrated in Fig. 2. To minimize losses we suppose that its longitudinal electric field component E_x has a zero crossing at the middle of the metal film. This implies that the transverse magnetic field H_y is symmetrical in the metal film and writes

$$H_y(x, z) = \begin{cases} H_0 \exp(ik_0 n_e x) \frac{\cosh[k_0 \sqrt{n_e^2 - \varepsilon_m} z]}{\cosh[k_0 \sqrt{n_e^2 - \varepsilon_m} h_m/2]}, & |z| \leq h_m/2 \\ H_0 \exp[ik_0 n_e x - k_0 \sqrt{n_e^2 - \varepsilon_s} (|z| - h_m/2)], & z \leq -h_m/2. \end{cases} \quad (\text{A11})$$

This gives the dispersion equation

$$\varepsilon_m \sqrt{n_e^2 - \varepsilon_s} + \varepsilon_s \sqrt{n_e^2 - \varepsilon_m} \tanh \left[\frac{k h_m}{2} \sqrt{n_e^2 - \varepsilon_m} \right] = 0. \quad (\text{A12})$$

The transverse magnetic field component H_y has the following distribution in the two upper media

$$H_y(x, z) = \begin{cases} H_0 \frac{\sin[k h_f \sqrt{\varepsilon_f - n_e^2} + \varphi]}{\sin \varphi} \exp[ik_0 n_e x - k_0 \sqrt{n_e^2 - \varepsilon_v} (z - z_0)], & z \geq z_0 = \frac{h_m}{2} + h_f \\ H_0 \exp(ik_0 n_e x) \frac{\sin \left[k \left(z - \frac{h_m}{2} \right) \sqrt{\varepsilon_f - n_e^2} + \varphi \right]}{\sin \varphi}, & \frac{h_m}{2} \leq z \leq z_0. \end{cases} \quad (\text{A13})$$

If we suppose that the longitudinal electric field component E_x has a zero crossing at the middle of the metal film, the needed thickness h_f may be found from the boundary conditions:

$$k h_f \sqrt{\varepsilon_f - n_e^2} = M \pi + \arctan \frac{\varepsilon_f \sqrt{n_e^2 - \varepsilon_c}}{\varepsilon_c \sqrt{\varepsilon_f - n_e^2}} - \arctan \frac{\varepsilon_f \sqrt{n_e^2 - \varepsilon_s}}{\varepsilon_s \sqrt{\varepsilon_f - n_e^2}}. \quad (\text{A14})$$

Using Eq. (A14) we can find the plasmon amplitude at the upper interface

$$|H(z_0)|^2 = \frac{\varepsilon_c^2 (\varepsilon_f - \varepsilon_s)}{\varepsilon_c^2 (\varepsilon_f - \varepsilon_s) + \varepsilon_f^2 (\varepsilon_s - \varepsilon_c)} |H_0|^2. \quad (\text{A15})$$

In the limit of large $|\varepsilon_m|$ we obtain from Eqs. (13) and (14)

$$S_0 \approx \frac{k_0^2 h_m}{2 \cos \theta} \frac{\varepsilon_c^2 (\varepsilon_f - \varepsilon_s)}{\varepsilon_s^2 (\varepsilon_f - \varepsilon_s) + \varepsilon_f^2 (\varepsilon_s - \varepsilon_c)}, \quad (\text{A16})$$

$$\Delta \theta \approx \frac{2\varepsilon_c^{5/2}}{\cos \theta} \left(\frac{k_0 h_m}{2} \right)^2 \frac{\text{Im}(\varepsilon_m)}{|\varepsilon_m|^2}, \quad (\text{A17})$$

$$R \sim \frac{1}{\varepsilon_e^{5/2} h_m} \frac{|\varepsilon_m|^2}{\text{Im}(\varepsilon_m)} \frac{\varepsilon_c^2 (\varepsilon_f - \varepsilon_s)}{\varepsilon_c^2 (\varepsilon_f - \varepsilon_s) + \varepsilon_f^2 (\varepsilon_s - \varepsilon_c)}. \quad (\text{A18})$$

ACKNOWLEDGMENTS

The authors want to express their gratitude to Professor V. A. Sychugov for his fundamental contribution to this work which owes much to his deep physical insight. The authors want to thank Dr. F. A. Pudonin for preparing the sandwiched structure with the ultrathin copper film and Professor Parriaux for his critical review of the manuscript. This work was supported partly by the Russian Foundation for Basic Research (Grant No. N98-02-17355), the Program of the Integration of the High School and Academical Science, and by the "Program International de Coopération Scientifique" (PICS 715).

¹D. Sarid, Phys. Rev. Lett. **47**, 1927 (1981).

²S. Glasberg, A. Sharon, D. Rosenblatt, and A. A. Friesem, Appl. Phys. Lett. **70**, 1210 (1997).

³I. F. Salakhutdinov, V. A. Sychugov, A. V. Tishchenko, B. A. Usievich, and F. A. Pudonin, IEEE J. Quantum Electron. **QE-34**, 1054 (1998).

⁴C. H. Liao, C. M. Lee, Y. T. Cheng, J. S. Shyu, and W. K. Su, Jpn. J. Appl. Phys., Part 1 **38**, 5938 (1999).

⁵N. M. Lyndin, I. F. Salakhutdinov, V. A. Sychugov, B. A. Usievich, F. A. Pudonin, and O. Parriaux, Sens. Actuators B **54**, 37 (1999).

⁶*Electromagnetic Surface Modes*, edited by A. D. Boardman (Wiley, New York, 1982).

⁷H. Raether, *Surface Plasmons on Smooth and Rough Surfaces and on Gratings*, Springer Tracts in Modern Physics (Springer, Berlin, 1988).

⁸H. A. Haus, *Waves and Fields in Optoelectronics* (Prentice-Hall, Englewood Cliffs, NJ, 1984), Chap. 7.2.

⁹G. A. Golubenko, A. A. Svakhin, V. A. Sychugov, and A. V. Tishchenko, Sov. J. Quantum Electron. **15**, 886 (1985).

¹⁰E. Popov and L. Mashev, Opt. Commun. **55**, 377 (1985).

¹¹D. Marcuse, IEEE J. Quantum Electron. **QE-9**, 958 (1973).

¹²H. H. Weetall, M. F. Mccurley, P. S. Cann, and J. Sambles, Sens. Actuators B **35**, 197 (1996).

¹³J. Chandezon, M. T. Dupuis, G. Cornet, and D. Maystre, J. Opt. Soc. Am. **72**, 839 (1982).

¹⁴D. W. Lynch and W. R. Hunter, in *Handbook of Optical Constant of Solids*, edited by E. D. Palik (Academic, Orlando, 1985), pp. 275–367.